Dual Circularly Polarized Antennas with
Low Cross-Polarization for GNSS-R Applications

Dual Circularly Polarized Antennas with Low Cross-Polarization for GNSS-R Applications

Yan Jia[1], Gianluca Dassano[2], Patrizia Savi[2]

1. Nanjing University of Posts and Telecommunications, Nanjing, China, jiayan521@gmail.com
2. Dept. of Electronic and Telecommunication (DET), Politecnico di Torino, Torino, Italy, patrizia.savi@polito.it

***Abstract*— Global Navigation Satellite System-Reflectometry (GNSS-R), has gained increasing interests as an efficient tool for remote sensing. It is based on the concept of utilizing the received signals reflected from the Earth's surface. Several GNSS-R system configurations were proposed depending on different retrieval algorithms. In a GNSS-R system, the antenna plays a key role as a receiving component.**

In this paper, in-situ measurements using a commercial dual circular polarized antenna receiving both the left-hand and right-hand circular polarization reflected from the ground are analyzed. A low cost and compact dual-port circular polarized patch antenna is designed and realized to overcome the limitations of the previous configuration. The prototype shows a low level of cross polarization suitable for GNSS-R application.

***Index Terms*—circular polarization, dual polarization, patch antenna, GNSS-R, remote sensing of soil.**

I. INTRODUCTION

In GNSS-Reflectometry (GNSS-R) technique, Global Navigation Satellite System (GNSS) signals are detected after reflection off the Earth's surface, the signal-to-noise ratio is evaluated and used to determine the properties of the surface remotely [1-6].

The majority of GNSS-R receivers operate in the L1 frequency band (1575.43 MHz) and use a circularly polarized antenna to receive the left-hand (LHCP) reflected from the Earth's surface [7,8]. In Fig. 1 the bi-static radar geometry of a typical GPSS-R ground receiver is shown. The receiver measures both the direct signal and the signal reflected from the Earth's surface. The direct signals transmitted by the GPS satellite are right-hand circularly polarized (RHCP), while the reflected signals are predominantly left-hand circularly polarized (LHCP) with very little RHCP components. Two antennas are generally mounted on the receiver, one RHCP, for the direct signal and the other LHCP to measure the reflected signals [9,10]. To simplify the GNSS-R system architecture and to improve its performance, a dual circular polarized antenna receiving both the left-hand and right-hand circular polarization with a low level of cross polarization is recommended [1].

The majority of the proposed dual-polarized patch antennas exhibit a linear polarization [8-10].

Several stacked patch antennas with circular polarization have been proposed but with a single polarization [7-9]. Dual polarization GNSS antennas were proposed but not so small and light weight as patch antennas [2,12,13]. In this work, in order to improve the performance of GNSS-R systems, we focus on the use of dual-polarized antennas with a low level of cross polarization to measure the reflected signals. First, a commercial antenna is considered and tested with in-situ measurements. The reflected signal was processed with an open-loop approach, in order to obtain Delay Doppler Maps (DDMs) and the corresponding Delay Waveforms. The Signal-to-Noise Ratio (SNR) of the in-sight satellites was obtained from the received power.

Then, in order to reduce the cost and weight of the GNSS-R system, especially for UAV (Unmanned Aerial Vehicle) or drones applications, a more compact and low cost dual-polarized antenna is designed. The antenna is feed by a 90° hybrid branch-line coupler and special attention is paid to obtain a low-level of cross-polarization. This cheap antenna achieves the required GNSS-R specification at L1 band of 1575 MHz in terms of return loss 20 dB and a low cross-polarization level.

II. IN-SITU MEASUREMENTS

For GNSS-R applications it is very important to have an antenna with a cross polarization level between the right-hand channel and the left-hand channel lower than

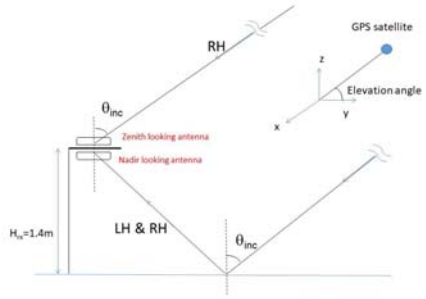

Figure 1. The basic architecture of GNSS-R system.

Figure 2. Measurement setup (left panel) and Antcom antenna (right panel).

-17dB [1]. During the SMAT project of Regione Piemonte, a customized antenna with -15dB of cross-polarization was made by Antcom and tested during several static measurements. In Fig. 1 the GNSS-R system used and the site (Grugliasco, Italy) are shown. The soil is 70% sand and it is covered by non-irrigated permanent meadows (see Table I for the soil characteristic). A standard RH antenna pointing to the sky was used for receiving the direct signal and the Antcom customized antenna was used to receive the reflected signals.

Given a satellite incident signal (right-hand polarized), from the bistatic radar equation, the coherent power scattered by the surface (left-hand polarized) is given by [11]:

$$P_{lr}^{coh} = R_{lr} \frac{P_t G_t G_r \lambda^2}{(4\pi)^2 (r_1 + r_2)^2} \quad (1)$$

where P_t is the transmitted signal power, G_t (G_r) is the transmitter (receiver) antenna gain; λ is the wavelength ($\lambda = 19.042$ cm for GPS L1 signal); r_1 is the distance between the receiver and the specular point, r_2 between the specular point and the satellite; R_{lr} is the power reflectivity which depends on the surface roughness as:

$$R_{lr}(\theta) = |\Gamma_{lr}(\theta)|^2 \chi(z) \quad (2)$$

where Γ_{lr} is the Fresnel reflection coefficient and $\chi(z)$ is the probability density function of the surface height z. Under the assumption of a perfectly flat surface, $\chi(z)=1$. Combining (1) and (2), the processed SNR of peak power can be written as:

$$SNR_{peak}^{refl} = \frac{P_{lr}^{coh} G_D}{P_N} = \frac{P_t G_t G_r \lambda^2 G_D}{(4\pi)^2 (r_1 + r_2)^2 P_N} |\Gamma_{lr}|^2 \quad (3)$$

where P_N is the noise power and G_D is the processing gain due to the de-spread of the GPS C/A code. The SNR peak power of the direct RHCP signal is:

$$SNR_{peak}^{dir} = \frac{P_t G_t G_r \lambda^2 G_D}{(4\pi)^2 r_3^2 P_N} \quad (4)$$

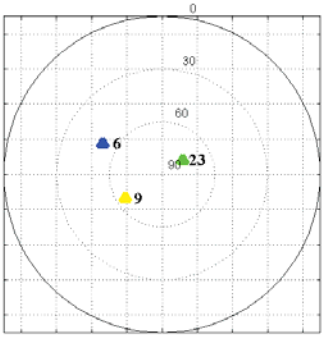

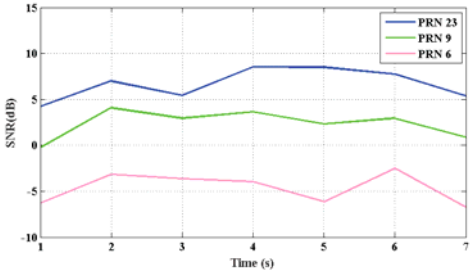

Figure 3. Sky-plot (top). SNR for PRN23, PRN9 and PRN6 (Bottom).

where r_3 is the distance between the transmitter and receiver. It has to be noted that the receiver gain G_r and noise power P_N of the direct signal (4) are not equal to those in (3) for the reflected signal. Therefore, a calibration process is needed. The ratio of the reflected SNR (3) over the direct SNR (4) is given by:

$$\frac{SNR_{peak}^{reflect}}{SNR_{peak}^{direct}} = \frac{r_3^2}{(r_1 + r_2)^2} |\Gamma_{lr}|^2 C \quad (5)$$

where C is a calibration parameter summarizing the uncertainties of G_r and P_N. The reflection coefficient Γ_{lr} can be written as a linear combination of vertical and horizontal polarization Fresnel coefficients (Γ_{vv}, Γ_{hh}) that are a function of the angle of incidence and the complex permittivity of soil. For satellites with high elevation angles $|\Gamma_{vv}| = |\Gamma_{hh}|$, the real part of the permittivity can be obtained by solving the equation for Γ_{vv}.

An example of SNR is shown in Fig. 3. As it was expected, higher elevation satellites (PRN23, 80° > PRN9, 70° > PRN6, 54 °) corresponds to higher SNR. The dielectric constant was then evaluated from the LH reflected signal and compared with local measurements using a TDR (Time Domain Reflectometry) system. Results are shown in Table II. As it was expected, the values of permittivity are close to the results obtained with TDR measurement only in the case of satellites with an elevation angle greater than 60° (PRN 23, PRN 9).

TABLE I. COMPOSITION OF THE SOIL IN GRUGLIASCO SITE.

Coarse Sand (%)	Fine Sand (%)	Very Fine Sand (%)	Coarse Silt (%)	Fine Silt (%)	Clay (%)	Organic Matter (%)
15.5	50.1	16.1	5.3	8.2	4.8	1.4

TABLE II. PERMETTIVITY COMPUTATION.

PRN 23			PRN 9			PRN 6		
Ele (deg)	SNR (dB)	$\mathcal{E}$	Ele (deg)	SNR (dB)	$\mathcal{E}$	Ele (deg)	SNR (dB)	$\mathcal{E}$
77.7	6	6	63.2	3	5	50.5	-5	2

The weight and cost of this antenna are not suitable for applications on UAV (Unmanned Aerial Vehicle) or drones. Therefore, we designed a microstrip patch antenna on FR4 with a low level of cross-polarization fulfilling the requirements of being cheap and lightweight.

III. COMPACT ANTENNA DESIGN AND SIMULATION

The proposed antenna is composed of a two-layer stacked patch and a hybrid branch-line coupler to realize RHCP and LHCP simultaneously. The stacked structure was chosen to obtain a low level of cross polarization and a wider bandwidth. The antenna works at L1 (1575 MHz) and its geometry is shown in Fig. 4. The two substrates are FR4 of dimensions 80x80mm. The top layer is 0.8 mm thick. The bottom layer is 1.6 mm. Square patches were considered to facilitate the fabrication process. The size of the top patch is 35x35 mm. The size of the patch sandwiched between the FR4 layers (42.5mm) is calculated in order to obtain the resonance at the operation band [14,15]. The probe-fed is designed for a good impedance matching and it plays a key role in the bandwidth definition.

The hybrid branch-line coupler is a symmetric structure and the left or right circular polarization can be obtained by simply changing the coupler's feeding. In fact, two orthogonal modes are excited by 90° phase difference resulting in CP radiated waves with a wide axial ratio bandwidth.

Ansoft HFSS software was used to simulate and optimize the whole antenna. The optimized parameters are

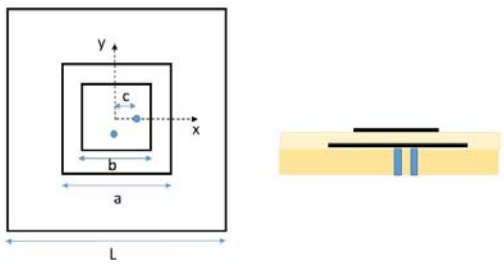

Figure 4. The geometry of the dual CP patch.

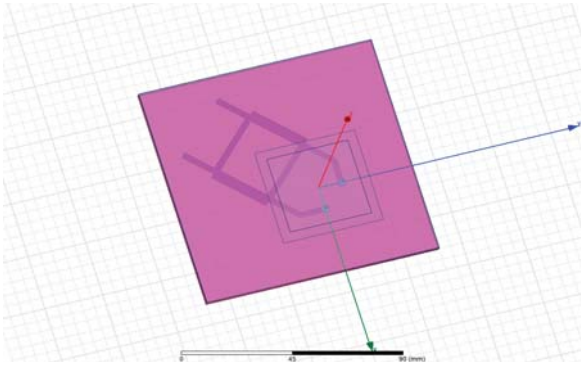

Figure 5. The geometry of proposed antenna modeled with HFSS.

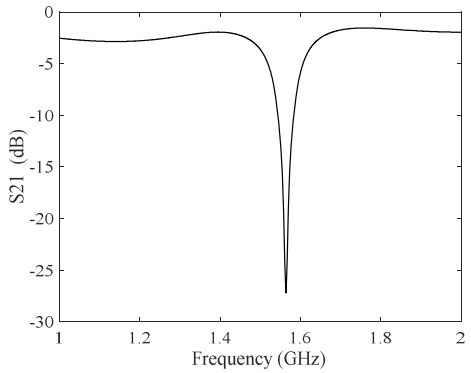

Figure 6. Simulations of the hybrid coupler isolation..

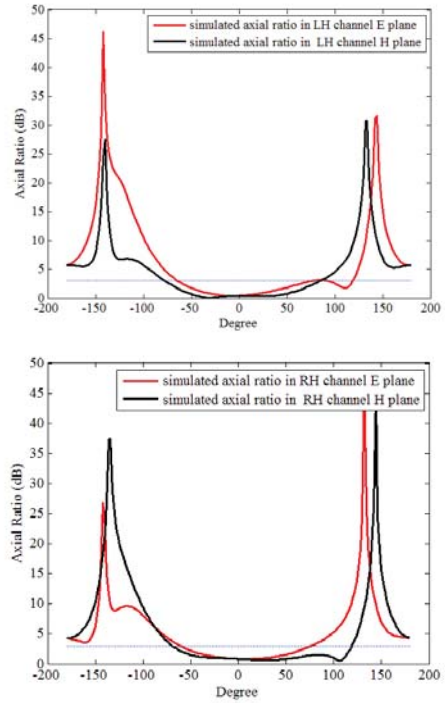

Figure 7. Axial rato LH and RH evaluated at f=1.575GHz.

Figure 8. Prototype of the dual polarized antenna.

a=43 mm, b=35mm, c=10mm, and L=80mm. The isolation of the two ports of the hybrid coupler was simulated and the result is shown in Fig. 6 and the axial ratio evaluated at 1.567 GHz is shown in Fig. 7. The radiated efficiency is affected mainly by the surface wave, dielectric losses and metallic losses. In this prototype due to the presence of two layers of FR4 and that one of the antennas is sandwiched between the two substrates, the radiated efficiency is not very high.between the two substrates, the radiated efficiency is not very high.

IV. COMPACT ANTENNA PROTOTYPE

This antenna was realized as shown in Fig. 8 and the return loss and radiation pattern measured in an anechoic chamber. In Fig. 9 the measured and simulated return loss

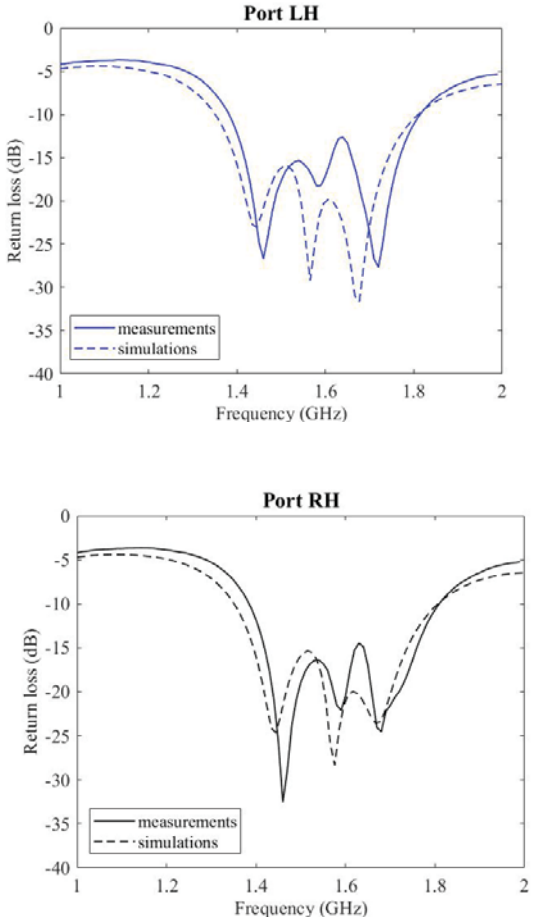

Figure 9. Comparison of simulated and measured S11 parameter of port LH and port RH.

of port LH and RH are compared. At the operating frequency (1575 MHz) the return loss is 18 dB for port LH and 23 dB for port RH. Both ports have -15 dB return loss in the range 1.41-1.78 GHz (bandwidth 370 MHz). The radiation pattern (simulation and measurements) of RH port and LH port are shown in Fig. 10 and 11, respectively (A-plane correspond to $\phi = 0^o$ and B-plane to $\phi = 90^o$, see the reference system of Fig. 4). These results shows a cross-polarization level satisfying the GNSS-R system requirements.

The cross-polarization level is lower around 50^o than in the boresight direction. But, considering the reflected link, the cross-polarization in the boresight direction ($\theta = 0^o$) is not very important. The antenna is used to receive the signals reflected from the ground and the power contributing to the SNR is coming from angles ranging from 10^o to 50^o.

V. CONCLUSION

A dual circular polarized stacked patch antenna was designed for GNSS-R applications. A key feature in the design was to add a lower dielectric constant substrate and a parasitic patch to obtain a low level of cross-polarization. The low cost and weight make this antenna useful for portable GNSS-R applications.

ACKNOWLEDGEMENT

This work was supported in part by the SMAT-F2 project of Regione Piemonte.

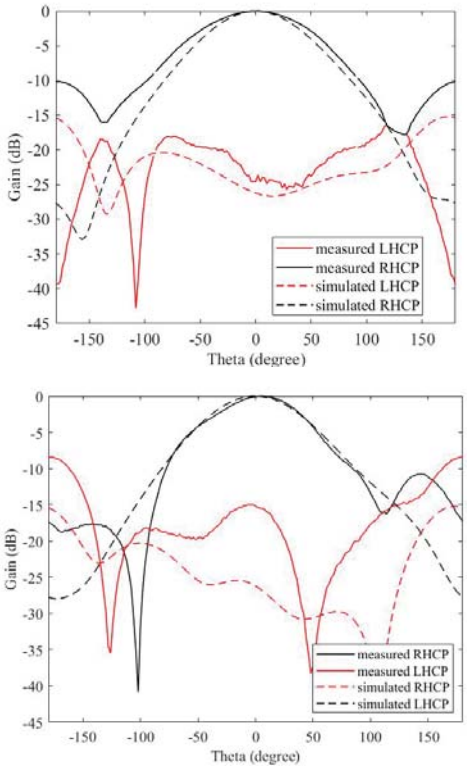

Figure 10. Radiation Pattern RH port. A-plane (top panel), B-

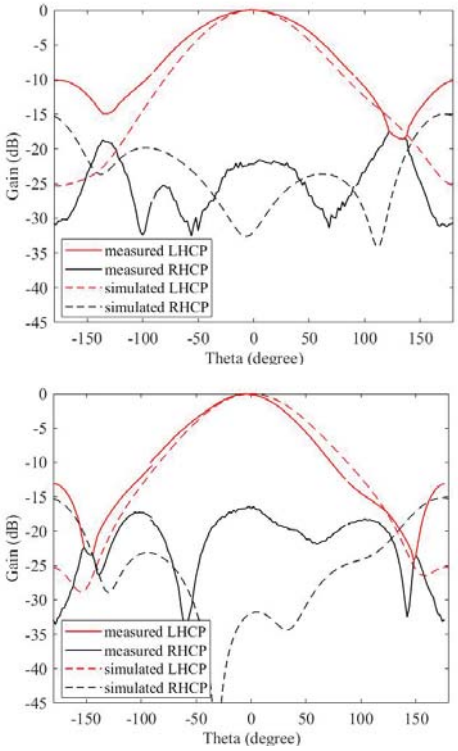

Figure 11. Radiation Pattern LH port. A-plane (top panel), B-plane (bottom panel).

REFERENCES

[1] S. J. Katzberg, O. Torres, M. S. Grant, and D. Masters, "Utilizing calibrated GPS reflected signals to estimate soil reflectivity and dielectric constant: Results from SMEX02," Remote sensing of environment , vol. 100, no. 1, pp. 17-28, 2006.

[2] K.M. Larson, J. J. Braun, E. E. Small, V. U. Zavorotny, E. D. Gutmann, and A. L. Bilich, "GPS multipath and its relation to near-surface soil moisture content," IEEE Journal of Selected Topics in Applied Earth Observations and Remote Sensing vol. 3, no. 1, pp. 91-99, 2010.

[3] N. Rodriguez-Alvarez, A. Camps, M. Vall-Llossera, X. Bosch-Lluis, A. Monerris, I. Ramos-Perez, E. Valencia et al, "Land geophysical parameters retrieval using the interference pattern GNSS-R technique," IEEE Transactions on Geoscience and Remote Sensing, vol. 49, no. 1, pp. 71-84, 2011.

[4] A. Egido, M. Caparrini, G. Ruffini, S. Paloscia, E. Santi, L. Guerriero, P. N. Pierdicca, N. Floury, "Global Navigation Satellite Systems Reflectometry as a Remote Sensing Tool for Agriculture." Remote Sens. 4, pp. 2356-2372, 2012.

[5] S.G. Jin, E Cardellach, F Xie, GNSS Remote Sensing, Theory, Methods and Applications. Springer, 2014.

[6] H. Carreno-Luengo, A. Amèzaga, D. Vidal, R. Olivé, J. F. Munoz, and A. Camps, "First polarimetric GNSS-R measurements from a stratospheric flight over boreal forests," Remote Sensing, vol. 7, no. 10, pp. 13120-13138, 2015.

[7] Y. Zhou, S. Koulouridis, G. Kizitas, and J. L. Volakis, "A novel 1.5 quadruple antenna for tri-band GPS applications," IEEE Antennas Wireless Propag. Lett., vol. 5, pp. 224–227, 2006.

[8] Y. Zhou, C.C.Chen, and J. L. Volakis, "Dual band proximity-fed stacked atch antenna for tri-band GPS applications," IEEE Trans. Antenna Propag., vol. 55, no. 1, pp. 220–223, Jan. 2007.

[9] A. E. Popugaev, R.Wansch, and S. Urquijo, "A novel high performance antenna for GNSS applications," in Proc. EuCAP07, pp. 1–5, 2007.

[10] S. Jin, G. P. Feng, and S. Gleason, "Remote sensing using GNSS signals: Current status and future directions," Advances in space research, vol. 47, no. 10, pp. 1645-1653, 2011.

[11] Y. Pei, R. Notarpietro, P. Savi, F. Dovis, ``A Fully Software GNSS-R receiver for Soil Monitoring", International Journal of Remote Sensing, vol. 35, no. 6, pp. 2378-2391, 2014.

[12] Y. Jia, P. Savi, D. Canone, R. Notarpietro, "Estimation of surface characteistics using GNSS LH-reflected signals: Land versus water," IEEE Journal of Selected Topics in Applied Earth Observations and Remote Sensing, vol. 9, no. 10, pp. 4752-8, 2016.

[13] Y. Jia, P. Savi, "Sensing soil moisture and vegetation using GNSS-R polarimetric measurement," Advances in Space Research, pp. 858-869, 2017.

[14] S. Gupta, M. Ramesh and Kalghatgi, "Parametric studies on isolation in probe-fed dual polarised microstrip antennas", Proc. European Conf. on Wireless Technologies, Oct. 2005.

[15] J. Anguera, C. Puente, C. Borja, N. Delbene, and J. Soler, "Dual frequency boradband stacked microstrip patch antennas," IEEE Antennas Wireless Propag. Lett., vol. 2, pp. 36-39, 2003.